AIP | Applied Physics Letters

Phosphor-free nanopyramid white light-emitting diodes grown on { 10 1 ¯ 1 } planes using nanospherical-lens photolithography

Kui Wu, Tongbo Wei, Ding Lan, Xuecheng Wei, Haiyang Zheng, Yu Chen, Hongxi Lu, Kai Huang, Junxi Wang, Yi Luo, and Jinmin Li

Citation: Applied Physics Letters **103**, 241107 (2013); doi: 10.1063/1.4840137
View online: http://dx.doi.org/10.1063/1.4840137
View Table of Contents: http://scitation.aip.org/content/aip/journal/apl/103/24?ver=pdfcov
Published by the AIP Publishing

Phosphor-free nanopyramid white light-emitting diodes grown on {10$\bar{1}$1} planes using nanospherical-lens photolithography

Kui Wu,[1,2] Tongbo Wei,[1,a)] Ding Lan,[3] Xuecheng Wei,[1] Haiyang Zheng,[1] Yu Chen,[1] Hongxi Lu,[1] Kai Huang,[4] Junxi Wang,[1] Yi Luo,[2] and Jinmin Li[1]
[1]*State Key Laboratory of Solid-State Lighting, Institute of Semiconductors, Chinese Academy of Sciences, Beijing 100083, China*
[2]*Department of Electronic Engineering, Tsinghua National Laboratory for Information Science and Technology/State Key Lab on Integrated Optoelectronics, Tsinghua University, Beijing 100084, China*
[3]*National Microgravity Laboratory, Institute of Mechanics, Chinese Academy of Sciences, Beijing 100080, China*
[4]*Platform of Characterization & Test, Suzhou Institute of Nano-tech and Nano-bionics, Chinese Academy of Sciences, Suzhou 215000, China*

(Received 29 March 2013; accepted 19 November 2013; published online 10 December 2013)

We reported a high-efficiency and low-cost nano-pattern method, the nanospherical-lens photolithography technique, to fabricate a SiO_2 mask for selective area growth. By controlling the selective growth, we got a highly ordered hexagonal nanopyramid light emitting diodes with InGaN/GaN quantum wells grown on nanofacets, demonstrating an electrically driven phosphor-free white light emission. We found that both the quantum well width and indium incorporation increased linearly along the {10$\bar{1}$1} planes towards the substrate and the perpendicular direction to the {10$\bar{1}$1} planes as well. Such spatial distribution was responsible for the broadband emission. Moreover, using cathodoluminescence techniques, it was found that the blue emission originated from nanopyramid top, resembling the quantum dots, green emission from the InGaN quantum wells layer at the middle of sidewalls, and yellow emission mainly from the bottom of nanopyramid ridges, similar to the quantum wires. © *2013 AIP Publishing LLC*. [http://dx.doi.org/10.1063/1.4840137]

GaN-based white light emitting diodes (LEDs) have been leading to a revolution in solid-state lighting and display backlight, for its low energy consumption and long life bearing.[1] The most widely used approach to generate white light using LEDs is blue LED with yellow phosphors.[2] However, this method has some disadvantages, such as low color-rendering index (CRI), Stokes shift energy loss, and degradation of phosphors which bring a relatively short life-time for LEDs.[3,4] Therefore, the most promising phosphor-free white light LEDs, such as a broad spectral width luminescence of nanorod-based LEDs, have been proposed to realize low-cost monolithic white light emissions.[5–8] In comparison to the conventional thin film LEDs, core/shell nanorod structure LEDs have higher aspect ratio and larger active regions. Besides, the InGaN/GaN multi-quantum wells (MQWs) grown on nonpolar or semipolar GaN facets are suggested to be able to effectively increase the light extraction efficiency and reduce the quantum confined stark effect (QCSE), which increases the internal quantum efficiency of LEDs through enhancing the radioactive recombination rate in MQWs.[9–12]

Recently, selective area epitaxy (SAE)[13] is a promising technique in creating semipolar GaN facets to fabricate core/shell LEDs. Conventionally, there are several semipolar planes can be obtained in the epi-growth, such as {10$\bar{1}$1}, {10$\bar{1}$3}, and {11$\bar{2}$2}.[14–18] In particular, the semipolar {11$\bar{2}$2} InGaN/GaN QWs grown by SAE method is supposed to realize a broad and multi-peak spectrum of white light LEDs, because of the nonuniform indium distribution on these facets under InGaN growth condition. The upper of the {11$\bar{2}$2} facet has more indium incorporation than the bottom and the emission red-shifts as the location moves toward the apex.[14] The {10$\bar{1}$1} planes are also promising for improving the performance of III-nitride light emitters owing to their reduced or even vanished polarization fields within the quantum wells.[15] However, for QWs on micro-size {10$\bar{1}$1} facets grown by SAE, the indium composition and thickness is uniform and the spectrum of this QWs possess only one luminescence peak.[17] Therefore, there are few reports on white LEDs grown on {10$\bar{1}$1} planes, not to speak of electrically driven ones. In this paper, we first use nanospherical-lens photolithography (NLP) to fabricate nano-patterned templates followed by the growth of the nanopyramid LEDs by applying SAE methods. Here, the NLP technology is a simple and economic process, using the single layer transparent polystyrene (PS) spheres as optical lenses to generate sub-wavelength holes on photoresist (PR) by focusing UV light.[19,20] Scanning electron microscopy (SEM), transmission electron microscopy (TEM), and cathodoluminescence (CL) measurements are performed to investigate the structural properties and the emission charactistics of the nanopyramid LEDs. It is found both the indium incorporation and the thickness of QWs from outer to inner layer along the [10$\bar{1}$1] orientations, increases little by little. Furthermore, the thickness and indium incorporation of QWs on the {10$\bar{1}$1} planes towards the substrate increase linearly. These nonuniform distributions result in the nanopyramid LEDs with broadband emission. As far as the

[a)]Author to whom correspondence should be addressed. Electronic mail: tbwei@semi.ac.cn. Tel.: +86-10-82305304. Fax: +86-10-82305245.

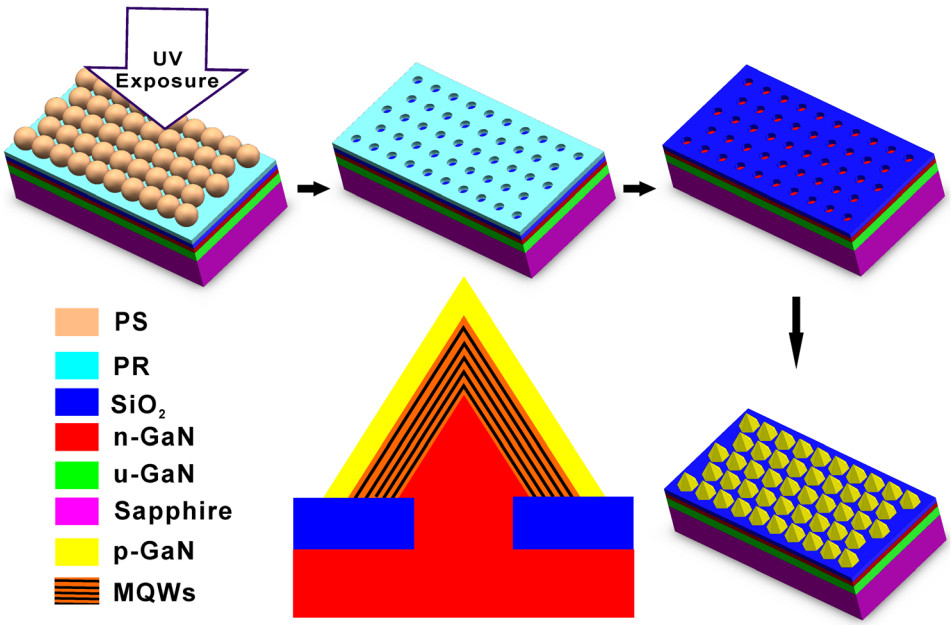

FIG. 1. Schematic illustrations of the process for fabricating phosphor-free nanopyramid white GaN LEDs by NLP method.

light emission of nanopyramid LEDs is concerned, the blue emissions are mainly owing to the nanopyramid top, quantum dots (QDs), green emissions to the InGaN QWs layer of the middle facets of sidewalls, and yellow emissions to the bottom of nanopyramid ridges, quantum wires (QWRs).

In our experiment, as shown in Fig. 1, a 2 μm n-GaN epitaxial layer was grown at 1050°, after the growth of a 30 nm GaN nucleation layer on c-plane (0001) sapphire substrates at 550 °C by metal organic chemical vapor deposition (MOCVD). A 400 nm thick SiO_2 layer was deposited on n-GaN using plasma enhanced chemical vapor deposition (PECVD) before the n-GaN template was coated by photosensitive resist (RF) AR-P 3120, followed by a hot plate bake for 15 min at 95 °C. Successively, nanospherical-lens was spin-coated on the RF, which was hexagonal closed-packed monolayer of PS spheres with a diameter of 900 nm. After exposure and developing process, air holes with a diameter of 400 nm on PR were fabricated. Subsequently, the patterned PR was baked at 110 °C for 10 min for bearing the following inductively coupled plasma (ICP) etching of SiO_2 dielectric. The ICP etching was performed using CF_4 (4 mTorr) at a radio-frequency power of 40 W, for duration 110 s by STS Multiplex AOE etching. SAE of GaN nanopyramid LEDs began with a 4 min growth of Si-doped n-GaN nanopyramid arrays with electron concentrations of 5×10^{18} cm^{-3}, which was equivalent to thin-film samples. The flows of the trimethylgallium and ammonia were chosen at a high V/III molar ratio of 12 000 in order to promote vertical growth to obtain nanopyramids with $\{10\bar{1}1\}$ facets, using hydrogen as a carrier gas. The total pressure and temperature were set to be 200 torr and 1055 °C, respectively. Then, the temperature was decreased to 740–780 °C for growing the active regions, with a V/III ratio of 4800 and a total pressure of 150 torr. The active regions consisted of an extra InGaN/GaN QW with narrow well (2 nm) and wide barrier (18 nm) which favored to the restrained effect, a five-period InGaN (3 nm)/GaN (8 nm) MQWs with uniform indium SCCM (SCCM denotes cubic centimeter per minute at STP). Finally, the growth parameters were set with a V/III ratio of 6000, and a total pressure of 130 torr to grow 20 nm p-$Al_{0.15}Ga_{0.85}N$ electron blocking layer and Mg-doped p-GaN cladding layers with a thickness of 30 nm.

Figure 2(a) shows the room temperature PL spectra of InGaN/GaN MQWs grown on the $\{10\bar{1}1\}$ facets of nanopyramids. They had demonstrated wide spectra of luminescence and white color emissions, as shown in the inset of Fig. 2(a), the optical microscope image taken from PL. As the growth temperature of QWs decreased from 780 °C to 740 °C, the PL peak intensity in short wavelength emission regions reduces gradually. On the contrary, this has been followed by a dramatic increase of the peak intensity of yellow emission regions. Here, the PL spectrum of MQWs grown at 740 °C is a little like the spectrum of sunlight, which is dominated by the yellow emissions of about 550 nm, the most sensitive wavelength to human eyes, as shown in Fig. 2(c). Correspondingly, the electroluminescent (EL) of this sample at 20 mA in Fig. 2(b) shows a white color emission, including the regions of blue, green, and yellow colors. The current–voltage (*I-V*) characteristic curve, illustrated in the upper of Fig. 2(b), is also investigated using the probe station connected with an ammeter and voltmeter. It is noteworthy that the curve shows the typical rectifying behavior of the LEDs, with a turn-on voltage of about 3 V. Furthermore, as shown in the lower region of Fig. 2(b), a schematic diagram of field distribution of the nanopyramid LEDs is presented, which shows the nature of current injection qualitatively. The black dotted lines and green arrows illustrate equipotential planes and hole carrier injection paths in the p-GaN capping layer of the nanopyramid LEDs under the turn-on voltage, respectively. Because of the high resistivity of p-GaN and the locally enhanced potential drop around the nanopyramid tips, the current channel is preferentially through the around nanopyramid tips of p-GaN capping layer. The tip, upper, and bottom of the nanopyramid LEDs, with different indium composition, were injected with different amount of current, which results in a broadband emission with main peak wavelength of about 550 nm.

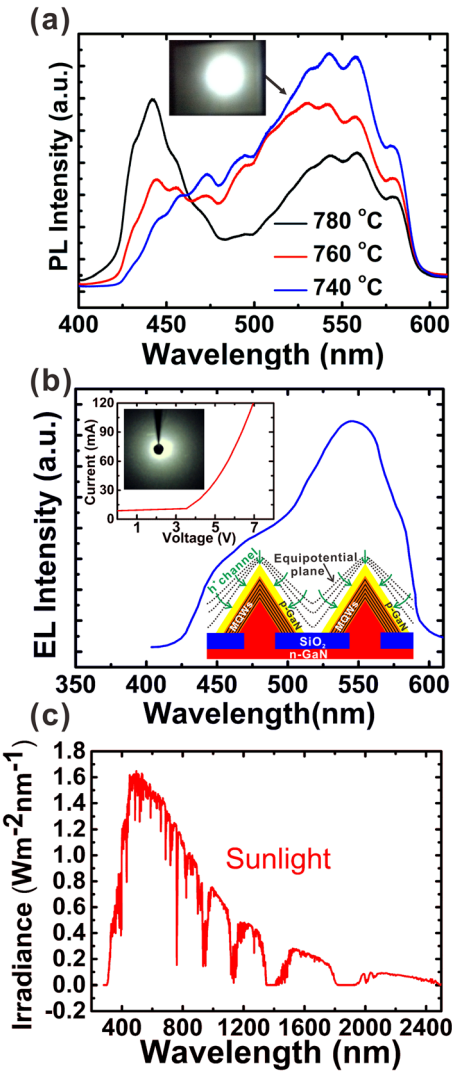

FIG. 2. (a) Room-temperature PL spectra from MQWs of nanopyramid LEDs grown on different temperatures, the inset showing the optical microscope image taken from PL measurement. (b) EL emission spectra of the LEDs at a driving current of 20 mA. The inset shows the current–voltage (*I-V*) characteristic curve and a schematic diagram of current distribution of the nanopyramid LEDs. (c) The sunlight spectra (the data from http://www.nrel.gov/rredc/solar_data.html).

At latter stage, we focus on the properties of the sample grown at 740 °C, with strong yellow emissions at about 550 nm.

Figure 3(a) shows the core of nanopyramid LEDs, a 4 min growth of Si-doped n-GaN on SiO_2 masked n-GaN templates. It can be seen that the core of nanopyramid LEDs is hexagonal and highly ordered with pyramid spires consisting of six equivalent semipolar $\{10\bar{1}1\}$ sidewalls arranged in a circle, as shown in Fig 3(a). On the core of nanopyramid n-GaN, active regions and p-GaN capping layer are grown, as shown in Fig. 3(b). After removing the SiO_2 mask, the mushroom shape nanopyramid LEDs was obtained, in Fig 3(c). Here, it is found that some nanopyramid LEDs are truncated with a small platform top, because the grown rate of Mg-doped GaN at the partially flat tops is lower than on the side facets. Thus, relatively thicker p-GaN is grown, to avoid the fact that the metallization have direct contact with the MQWs, which may cause electrical leakages. In Fig. 3(d), the cross-sectional TEM view of a nanopyramid LED

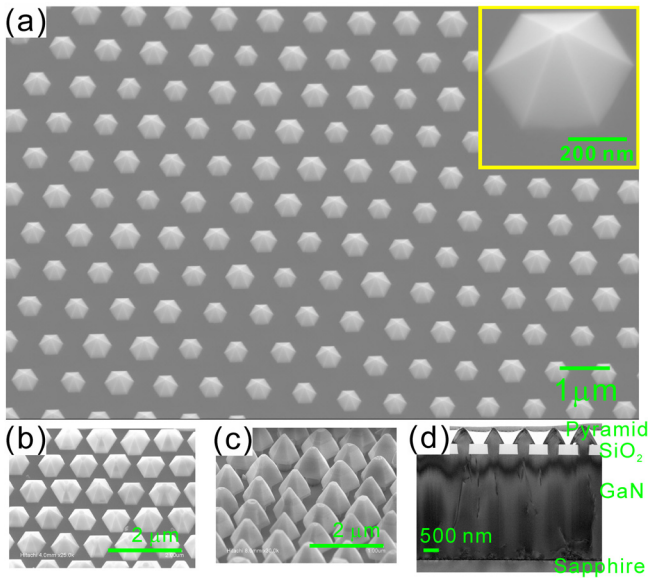

FIG. 3. Tilted SEM images of (a) nanopyramid core arrays before MQWs were regrown, (b) nanopyramid LED arrays with SiO_2 mask and (c) after removing SiO_2, respectively. (d) TEM cross section view of the nanopyramid LED arrays.

structure demonstrates a typical dislocation terminated below the SiO_2 mask. Therefore, these nanopyramids can be regarded as threading dislocation free, which is beneficial to reducing electrical leakage.[21]

To explore the nature of the broadband LEDs, the high-magnification cross-sectional TEM image of MQWs is demonstrated as shown in Fig. 4(a). The inclined sidewalls are clearly observed with an extra QW and five-period MQWs embedded, where no threading dislocation can be seen. Due to nanoscale epitaxy in confined hole-openings, no extended crystal defects can be observed, such as dislocations or stacking faults. The arrow shows the c-axis $\langle 0001 \rangle$ direction of wurtzite, and it is also the growth direction. The HR-TEM images in Figs. 4(b) and 4(c) show the upper and the bottom part of the single nanopyramid LED, respectively. In the TEM images, alternately stacked bright and dark layers, which are corresponding to the InGaN QWs and GaN quantum barriers (QBs) layers, are also clearly identified with clear interface due to the atomic mass contrast. The angle between the sidewall plane and the basal plane (0001) is measured to be 61.96°, showing that the sidewalls are corresponding to the $\{10\bar{1}1\}$ planes of wurtzite GaN. The diffraction pattern is also shown in the bottom panel of Fig. 4(b), taken along $[11\bar{2}0]$ zone axis. However, the MQWs at the tip of nanopyramid are geometric unsharpness, similar to that of quasi QDs. More information about thickness and indium distribution related to the embedded MQWs can be obtained from the HR-TEM and by measuring energy-dispersive X-ray (EDX) spectra, respectively, in Figs. 4(c)–4(g). In the solid line trapezoid, there is a section of ladder-shaped QW. Along the section of QW from (i) to (ii), the thickness and indium incorporation are linearly increased in Figs. 4(d) and 4(e) (the straight-line fitting results of black solid line in Fig. 4(d) and green one in Fig. 4(e)). The thickness with non-uniform (trapezoid) diameter continuously increases from about 2 nm to 4 nm from (i) to (ii), showing the fact that the growth rate on $\{10\bar{1}1\}$ planes is different from that on c

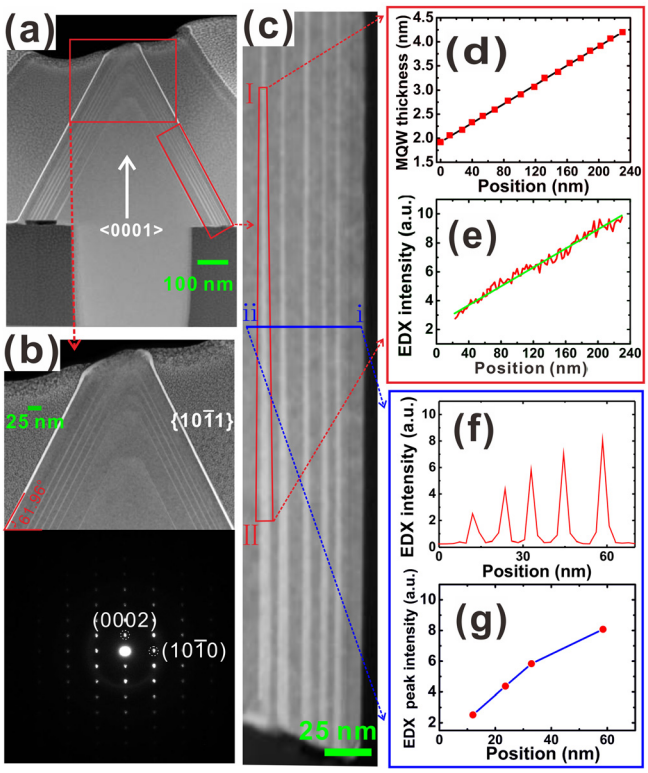

FIG. 4. (a) High-magnification cross-sectional TEM image of nanopyramid InGaN/GaN MQWs, taken along the [11$\bar{2}$0], solid arrow indicating the c axis. TEM images of MQWs formed on (b) upper (The inset shows the corresponding diffraction pattern of the nanopyramid LED), and (c) sidewall areas of the nanopyramid LEDs. The MQW thickness (d) and EDX line profiles (e) formed on (c) along the trapezoid QW (the solid straight lines shown the fitting curves). (f) The EDX intensity of MQWs for the scan line perpendicular to the sidewalls and (g) the corresponding EDX peak intensity.

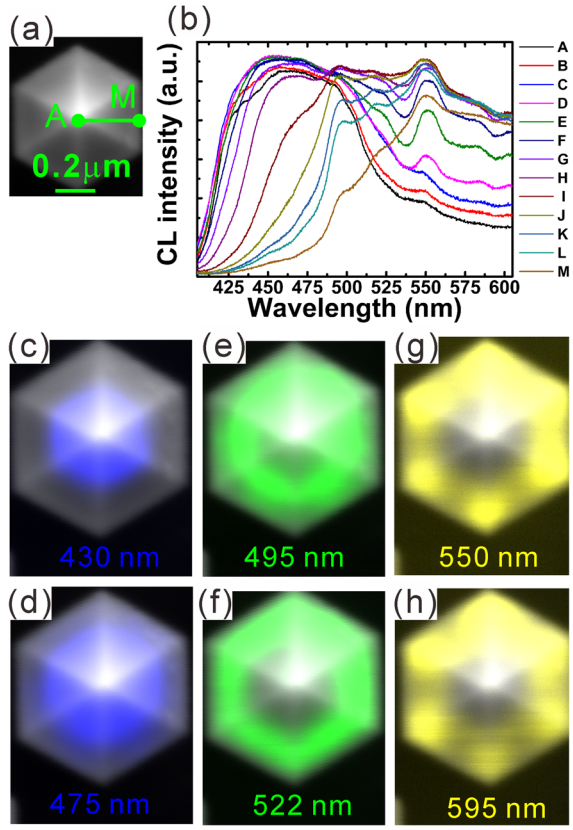

FIG. 5. (a) SEM images of a single nanopyramid from the apex (A) to the bottom (M) and (b) the corresponding CL spectrum of every localized position. (c)-(h) Monochromatic CL images at the given emission wavelength.

planes. When grown on c plane, there is a uniform quantum well thickness of 2 nm in the same growth time of that on {10$\bar{1}$1} planes. The indium composition along the sidewall QWs from the apex to the bottom of pyramids is definitely different from that on {11$\bar{2}$2} planes, on which the indium composition is decreased, according to the direction above.[14] Meanwhile, Figures 4(f) and 4(g) show the EDX line profiles of indium content in the five QWs, by measuring from (i) to (ii) of the line perpendicular to the sidewalls. The result shows that the indium concentration of $In_xGa_{1-x}N$ QW is about number of 11.7% increment than the upper adjacent one. The MQWs with different thickness and indium composition spatial distribution, which is associated with the difference in the arrival rate of growth species during MOCVD growth, may be responsible for the broadband emissions. However, this phenomenon has not been found on micro-size facets with {10$\bar{1}$1} planes.[14]

The CL-SEM analyzing for a single nanopyramid is taken at an acceleration voltage of 5 kV and at room temperature, providing the influence of the tapered MQWs thickness and indium composition spatial distribution on the optical properties of emission wavelength and intensity. CL linescans along the green dash line from A to M in Fig. 5(a) with spatial resolution about 50 nm are shown in Fig. 5(b). The emission wavelengths suffer from a strong red-shift, along the given direction from apex (A) to bottom (M) of the nanopyramid facets. The apex mainly belongs to blue emissions, the middle zone to blue-green emissions, and the bottom zone to yellow ones. The nonuniform emissions are attributed to the nonuniform InGaN MQWs on nanopyramid {10$\bar{1}$1} facets, which with varying thickness and composition along the given directions. Consequently, notable red-shift and relative intensity variations are observed. Interestingly, monochromatic CL images also show distinct spatial distribution of different wavelength emissions. In Figs. 5(c) and 5(h), the blue emissions around 430 nm is mainly attributed to the apex zones (QDs emissions), and the blue emissions around 475 nm originate the InGaN QWs from the upper-part of nanopyramid facets. The green emissions are localized at the middle of nanopyramid facets (QWs emissions) and the yellow ones are from the lower nanopyramid ridges (QWRs emissions). The information is consistent with the above results of TEM and EDX, and demonstrates the nature of the broadband emission LEDs.

In summary, we use the nanospherical-lens lithography technique, a high efficiency and low cost nano-pattern method, to fabricate SAE-used masked n-GaN templates. By controlling the growth temperatures, highly ordered hexagonal nanopyramid GaN LEDs are grown on {10$\bar{1}$1} planes. The phosphor-free nanopyramid LED demonstrates a broadband white light emissions due to the graded thickness and indium composition of the QWs. Using the CL analysis, we find that the blue emissions are mainly attributed to the apex (QDs), and the green emissions are from the QWs layer of the middle sidewalls, and the yellow emissions originate from the under-part of nanopyramid ridges (QWRs).

This work was supported by the National Natural Sciences Foundation of China under Grant Nos. 61274040 and 61274008, by the National Basic Research Program of China under Grant No. 2011CB301902, and by the National High Technology Program of China under Grant Nos. 2011AA03A103 and 2011AA03A105.

[1]S. Pimputkar, J. S. Speck, S. P. DenBaars, and S. Nakamura, Nat. Photonics **3**, 180 (2009).
[2]E. F. Schubert, T. Gessmann, and J. K. Kim, *Light Emitting Diodes* (Wiley Online Library, 2005).
[3]N. Kimura, K. Sakuma, S. Hirafune, K. Asano, N. Hirosaki, and R.-J. Xie, Appl. Phys. Lett. **90**, 051109 (2007).
[4]E. F. Schubert and K. Kim, Science **308**, 1274 (2005).
[5]Y.-H. Ko, J.-H. Kim, L.-H. Jin, S.-M. Ko, B.-J. Kwon, J. Kim, T. Kim, and Y.-H. Cho, Adv. Mater. **23**, 5364 (2011).
[6]T. Kim, J. Kim, M. S. Yang, S. Lee, Y. Park, U. I. Chung, and Y. Cho, Appl. Phys. Lett. **97**, 241111 (2010).
[7]H. P. T. Nguyen, K. Cui, S. F. Zhang, S. Fathololoumi, and Z. Mi, Nanotechnology **22**, 445202 (2011).
[8]H.-W. Lin, Y.-J. Lu, H.-Y. Chen, H.-M. Lee, and S. Gwo, Appl. Phys. Lett. **97**, 073101 (2010).
[9]P. Waltereit, O. Brandt, A. Trampert, H. T. Grahn, J. Menniger, M. Ramsteiner, M. Reiche, and K. H. Ploog, Nature **406**, 865 (2000).
[10]C.-Y. Cho, S.-H. Han, S.-J. Lee, S.-C. Park, and S.-J. Park, J. Electrochem. Soc. **157**, H86 (2010).
[11]C.-Y. Cho, I.-K. Park, M.-K. Kwon, J.-Y. Kim, S.-J. Park, D.-R. Jung, and K.-W. Kwon, Appl. Phys. Lett. **93**, 241109 (2008).
[12]S.-P. Chang, Y.-C. Chen, J.-K. Huang, Y.-J. Cheng, J.-R. Chang, K.-P. Sou, Y.-T. Kang, H.-C. Yang, T.-C. Hsu, and H.-C. Kuo, Appl. Phys. Lett. **100**, 061106 (2012).
[13]R. Colby, Z. W. Liang, I. H. Wildeson, D. A. Ewoldt, T. D. Sands, R. E. García, and E. A. Stach, Nano Lett. **10**, 1568 (2010).
[14]J.-R. Chang, S.-P. Chang, Y.-J. Li, Y.-J. Cheng, K.-P. Sou, J.-K. Huang, H.-C. Kuo, and C.-Y. Chang, Appl. Phys. Lett. **100**, 261103 (2012).
[15]T. Wunderer, P. Brückner, B. Neubert, F. Scholz, M. Feneberg, F. Lipski, M. Schirra, and K. Thonke, Appl. Phys. Lett. **89**, 041121 (2006).
[16]S. Srinivasan, M. Stevens, F. A. Ponce, H. Omiya, and T. Mukai, Appl. Phys. Lett. **89**, 231908 (2006).
[17]H. B. Yu, L. K. Lee, T. Jung, and P. C. Ku, Appl. Phys. Lett. **90**, 141906 (2007).
[18]M. Feneberg, F. Lipski, R. Sauer, K. Thonke, T. Wunderer, B. Neubert, P. Brückner, and F. Scholz, Appl. Phys. Lett. **89**, 242112 (2006).
[19]T. B. Wei, K. Wu, D. Lan, Q. F. Yan, Y. Chen, C. X. Du, J. X. Wang, Y. P. Zeng, and J. M. Li, Appl. Phys. Lett. **101**, 211111 (2012).
[20]W. Wu, A. Katsnelson, O. G. Memis, and H. Mohseni, Nanotechnology **18**, 485302 (2007).
[21]C. S. Xia, Z. M. S. Li, Z. Q. Li, and Y. Sheng, Appl. Phys. Lett. **102**, 013507 (2013).